Discovery, The Student Journal of Dale Bumpers College of Agricultural, Food and Life Sciences

Volume 8 Article 12

Fall 2007

A computational model for analysis of uncoupled NO synthase on nitric oxide and superoxide interaction in microcirculation

William Richardson
University of Arkansas, Fayetteville

Mahendra Kavdia
University of Arkansas, Fayetteville

A computational model for analysis of uncoupled NO synthase on nitric oxide and superoxide interaction in microcirculation

William J Richardson[*] *and Mahendra Kavdia*[†]

ABSTRACT

Nitric oxide (NO) produced by endothelial cells is a key component for blood-vessel dilation. Dilation is achieved through smooth muscle relaxation as a response to NO transport. Inhibition of this process occurs through the inactivation of NO by reactive oxygen species, especially superoxide (O_2^-). NO and superoxide react quickly, forming peroxynitrite ($ONOO^-$). Both superoxide and peroxynitrite apply oxidative stress on vascular tissue. Experimental studies investigating NO interactions are difficult since these reactions occur rapidly and over small distances. This study presents a computational model to describe the interactions of NO, superoxide, and peroxynitrite across an arteriole/venule pair. Based on principles of mass transport, and using knowledge of chemical concentrations and reaction rates, a mathematical model was developed to generate the concentration profiles for NO, O_2^-, and $ONOO^-$. We simulated excessive oxidative stress by uncoupled eNOS and determined its effect on NO concentration profiles throughout the region. Based on our understanding of the interactions involved, we predicted 1) increased oxidative stress in the venule decreases NO levels in regions of both the venule and neighboring arteriole, and 2) the amount of NO reduction will vary depending on the location of O_2^- increase. The model demonstrates that different sources of O_2^- have varied effects on NO concentration profiles, and excessive oxidative stress in the venule can impact NO levels in the venule as well as the arteriole. The results provide a more complete description of nitric oxide transfer, which is an important step toward understanding vascular complications in many pathological conditions.

[*] William Richardson is a senior majoring in biological engineering.

[†] Dr. Mahendra Kavdia is an assistant professor in the Department of Biological and Agricultural Engineering and the faculty mentor.

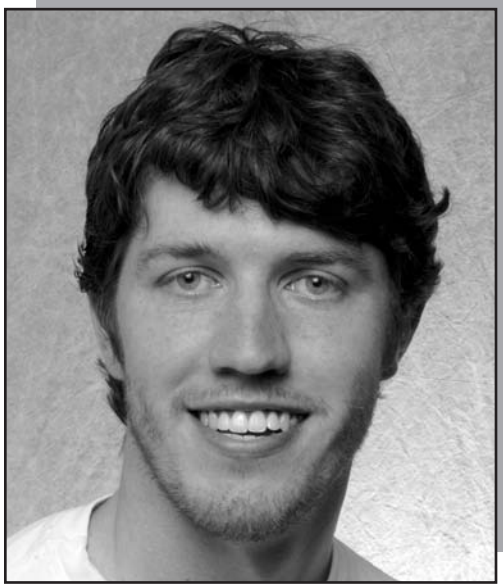

William J. Richardson

MEET THE STUDENT-AUTHOR

I graduated in May 2003 from Pulaski Academy in Little Rock, Ark. The following fall, I began my undergraduate studies at the University of Arkansas and was given the Governor's Distinguished Scholarship, the Chancellor's Scholarship, and the U.S. Army Corp of Engineers Scholarship. During my time at Arkansas, I have been involved with the University Concert Choir, Tau Beta Pi Honors Engineering Society, and the University Ultimate Frisbee Club Team.

I joined the department of Biological and Agricultural Engineering because of my interest in applying technology and design to problems associated with living systems. My career aim is to work in the medical field performing research and development involving medical devices. I became interested in doing a research project my junior year and began working with Dr. Kavdia on his studies of endothelial function and nitric oxide interactions in the vasculature. In May 2007, I graduated with honors and plan to attend graduate school, pursuing a Ph.D. in biomedical engineering. Conducting undergraduate research and submitting a thesis with Dr. Kavdia has helped to introduce me to academic research and has developed skills that will prove beneficial in my future efforts, both academically and professionally.

INTRODUCTION

Nitric Oxide (NO) plays a very important role in the human vasculature as a key element in the mechanisms involved in blood-vessel dilation (Bitar et al., 2005; Cook, 2006; Harrison et al., 2006). It is produced by several forms of the enzyme NO synthase (NOS). The most notable form is eNOS, located in the endothelial cells that line the inner surface of blood vessels (Cook, 2006). Shear stress caused by blood flow stimulates eNOS to oxidize the amino acid L-arginine and release NO into the surrounding tissues (Harrison et al., 2006). The target cells are smooth muscle cells where NO is used to convert GTP to cGMP (Cannon, 1998). The increase in cGMP level results in muscle relaxation and thus dilates the vessel.

Inhibition of this process occurs through impaired eNOS production of NO, as well as through inactivation of NO molecules by a number of reactive oxygen species (ROS) (Cook, 2006). The most significant ROS is superoxide (O_2^-), which reacts very quickly with NO to form peroxynitrite ($ONOO^-$) (Guzik et al., 2002; Vasquez-Vivar et al., 1998). Both O_2^- and $ONOO^-$ create oxidative stresses in vascular tissues and have a number of harmful effects, such as enzyme inhibition and lipid peroxidation (Kavdia, 2006).

Oxidative stress is exacerbated under pathological conditions such as diabetes, atherosclerosis, and hypertension where O_2^- levels are increased in particular regions of the vasculature, thus decreasing NO availability (Cannon, 1998; Li and Shah, 2004; Wood et al., 2006). Depending upon the condition, the source of ROS varies, and thus the location of oxidative stress also varies. A major source of superoxide during dysfunctional conditions is "uncoupled" eNOS. "Uncoupled" nitric oxide synthase refers to the eNOS enzyme when it is generated with an oxidized form of its normal cofactor, tetrahydrobiopterin (BH_4) (Bitar et al., 2005; Harrison et al., 2006). This results in a change in the NO production mechanism as discussed by Li and Shah (2004), and causes eNOS to produce superoxide rather than NO. Under increased oxidative stress during pathophysiological conditions, BH_4 is oxidized more readily, resulting in greater concentrations of uncoupled eNOS and thus creating even greater levels of superoxide.

During normal conditions, oxidative stress is kept in balance by antioxidants such as superoxide dismutase (SOD) and carbon dioxide. SOD consumes O_2^-, converting it to less harmful oxygen compounds, and CO_2 reacts with peroxynitrite, limiting its availability (Kavdia, 2006: Taniyama and Griendling, 2003). A knowledge of interactions between NO, superoxide, and

peroxynitrite, along with molecules such as SOD and CO_2, is crucial to understanding endothelial function and dysfunction. Impact of nearby vessels on NO transport and endothelial function has also been shown. A number of recent studies report that NO produced in the venule can cause dilation of the adjacent arteriole and similarly, NO produced in the arteriole can cause dilation of the paired venule (Guzik et al., 2002; Kavdia, 2006). Increased O_2^- in the venular wall can impact NO concentrations in both the venule and the neighboring arteriole. Thus, it is important to consider a venule presence in the vicinity of an arteriole when studying NO and O_2^- interactions.

These reactions occur rapidly and over very small distances, thus testing proves to be difficult. We took a computational approach to study NO and superoxide interactions. The computer model used was based on principles of mass transport. Currently, models exist that consider an arteriole-venule pairing so as to examine NO transport (Kavdia and Popel, 2006), and models exist that consider NO, O_2^-, and $ONOO^-$ interactions so as to examine NO transport (Kavdia, 2006). Our model combines both of these approaches to establish a more complete description of nitric oxide transport in the microvasculature, in the presence of oxidative stress.

MATERIALS AND METHODS

Model geometry. The geometry of our model has been presented previously by Kavdia and Popel (2006) and consists of a tissue containing a paired arteriole and venule as seen in Fig. 1. Each blood vessel has six regions: red blood cell-rich (CR) and red blood cell-free (CF) regions in the lumen, endothelium (E), interstitial space (IS) between the endothelium and smooth muscle layers, smooth muscle (SM), and a nonperfused parenchymal tissue (NPT). These regions are modeled as concentric circles of increasing radii. Vessels are surrounded by a parenchymal tissue (PT) region, assumed to be perfused with capillaries that distinguish it from the NPT. The CR luminal region is assumed to be a homogeneous solution of red blood cells. The PT region represents a homogeneous tissue of capillaries and parenchymal cells (Kavdia, Tsoukias, and Popel, 2002).

As the main production of NO occurs in the endothelial cells by eNOS, NO production is modeled using boundary conditions on the luminal and abluminal surfaces of the endothelial region. Superoxide production in the endothelium is also modeled as surface release incorporated as boundary conditions. In the other regions, O_2^- generation is included as an overall rate of production. Peroxynitrite is produced only by reaction of NO and O_2^- and is considered to occur in all regions.

In deriving mass balance of the three species (NO, O_2^-, and peroxynitrite), the convective transport term was neglected due to the speed of the reactions (Buerk, et al., 2003). Also, concentration profiles have been shown to reach steady state very quickly (Tsoukias et al., 2004). Therefore, mass transport of the species throughout vascular tissues was described using the steady-state mass transport equation (Equation 1). Written in cylindrical coordinates,

$$D_j \nabla^2 C_j \pm \sum R_{j,i} = 0 \qquad (1)$$

where $_j$ represents the particular molecule of interest; C_j is concentration; D_j is diffusivity; and $R_{j,i}$ stands for production and consumption of the species due to chemical reactions.

Total concentration of peroxynitrite includes concentrations of $ONOO^-$ and peroxynitrous acid (ONOOH) (Nalwaya and Deen, 2003). ONOOH is in acid-base equilibrium with $ONOO^-$.

Boundary Conditions. Continuities of NO, O_2^-, and peroxynitrite mass transport were imposed at each interface between the regions except for the outer edge of the geometry and the surfaces of the endothelium. At the outer edge of the PT, a zero-flux boundary condition was fixed, and at the interfaces with the endothelium, the release of NO and O_2^- were given by Equations 2a and 2b.

$$Q_j = D_j \frac{\partial C_{j,cf}}{\partial r} - D_j \frac{\partial C_{j,en}}{\partial r} \qquad (2a)$$

$$Q_j = D_j \frac{\partial C_{j,cf}}{\partial r} - D_j \frac{\partial C_{j,en}}{\partial r} \qquad (2b)$$

where $_j$ stands for NO and O_2^-, and Qj represents half of the total release of either species from the endothelium. Both arteriolar and venular endothelial productions were modeled with these equations.

Chemical Reactions. Chemical interactions that were taken into account for the sum of reactions term in Equation 1 vary between regions as each tissue is assumed to be composed of different types of cells. However, all reactions present in the arteriole are considered to be present in similar regions of the venule. In the cell rich region, NO is consumed by hemoglobin contained in red blood cells as a function of the NO concentration, reaction rate with RBC hemoglobin, hemoglobin concentration, and hematocrit. In the smooth mus-

cle region, NO reacts with sGC according to a second-order reaction. In the parenchymal tissue region, NO is consumed and produced by capillaries, according to capillary hematocrit, and capillary volume. Thus O_2 reacts with NO in the CF, EN, IS, and NPT regions in a second-order reaction in NO concentration.

In all regions, NO reacts with O_2^- to produce peroxynitrite, O_2^- is consumed by SOD, and peroxynitrite is consumed by CO_2. The reaction-rate expressions for all reactions are presented in Table 1.

Parameter Values. Parameters used in the model are listed along with their values in Table 1. Reasoning for the chosen geometries have been described in detail in previous reports (Kavdia and Popel, 2004; Kavdia and Popel, 2003). A ratio of 0.5 is assumed for the arteriole-to-venule radius values because of reported findings of roughly 0.4-0.5 ratios (Boegehold, 1996; Nellore and Harris, 2004). Diffusivities of NO, O_2^-, and peroxynitrite are assumed to be constant across the geometry and equal 3.3 x 10^{-5}, 2.8 x 10^{-5}, and 2.6x 10^{-5} cm^2/s, respectively (Nalwaya and Deen, 2003; Zacharia and Deen, 2005).

Reaction rate for consumption of NO in the CR region is 1,270 s^{-1} (Kavdia and Popel, 2006). This value is a product of the reaction rate of NO with hemoglobin, heme concentration of 20.3 mM in a single red-blood cell, and a hematocrit of 0.45. Capillary contribution to NO is calculated using a hematocrit of 0.3 and fractional volume of 0.0146 (Ellsworth, Popel, and Pittman, 1988; Kavdia and Popel, 2006). The resulting reaction rate is k_{cap} = 12.4 s^{-1}.

NO production is located in the arteriolar and venular endothelia, as well as in the capillary wall and is considered equal (per unit surface area) in these regions. A value of 2.65 x 10^{-12} mol/cm^2-s is half of the total NO production rate, and is therefore used for each side of the endothelium (Malinski et al., 1993). The corresponding release rate from the capillary region is 8.6 x 10^{-7} M/s.

Release of superoxide is assumed to be 1.72 x 10^{-7} M/s (20% of NO production) across the whole geometry, excluding the lumen. This is also the surface release rate from endothelial regions. Peroxynitrite equilibrium with peroxynitrous acid is described in the model according to the fraction f, which equals 1/ $(1+10^{pK_{per}-pH})$ with K_{per} = 6.75 (Nalwaya and Deen, 2003). Values for pH in the lumen and the vessel walls are assumed to be 7.4 and 7.0, respectively.

Numerical solution. The system of differential equations generated with equation 1 for NO, O_2^-, and $ONOO^-$ was solved using Flex PDE 3.0 software (PDE Solutions, Inc., Antioch, Calif.). We used this software as it has a meshing algorithm that produces a greater amount of elements when the concentration gradient is larger. An adaptive meshing with a relative accuracy of 0.001 was used for the numerical solutions.

Simulations. Profiles for chemical species were generated according to the concentration values along the horizontal center axis of the geometry, and extended 350 μm (100 μm left of the arteriole to 150 μm right of the venule). Along with the base case parameters under normal conditions, the model was used to simulate uncoupled nitric oxide synthase. It has been reported that uncoupled eNOS produces levels of NO approximately 1/3 x the base case scenario and levels of superoxide approximately 3 x the base case (Shinozaki et al., 1999; Vasquez-Vivar et al., 1998). Therefore, to model the impact of eNOS uncoupling, the endothelial surface release rates of NO and O_2^- were multiplied by factors of 1/3 and 3, respectively.

RESULTS AND DISCUSSION

Base case steady state concentration profiles for NO, superoxide, and peroxynitrite. For the base case, we used normal parameters as described in the methods section. Plots of NO, O_2^-, and per concentrations for the base case are displayed in figures 2, 3, and 4, respectively. All species reached steady state values within 100 μm of the vessel centers as they proceeded through the vessel walls and into the parenchymal tissue region. These values equal 66.3, 0.084, and 0.88 nM for NO, superoxide, and per concentrations, respectively. Concentration peaks were located in the endothelial regions with a max NO equaling 98.7 nM and occurring in the arteriolar endothelium distal to the venule; max O_2^- equaling 1.6 nM and occurring in the venular endothelium distal to the arteriole; and max per equaling 3.8 nM and occurring in the arteriolar endothelium proximal to the venule. Concentration gradients are steep on either side of endothelial peaks and drastically decrease in the lumen. NO and O_2^- are completely consumed, and per is reduced to 0.014 nM in the venular lumen and 0.52 in the arteriolar lumen.

Uncoupled eNOS impact. We examined the effects of uncoupled nitric oxide synthase on concentration profiles of NO, superoxide, and peroxynitrite by changing surface release parameters at the endothelial regions. Superoxide production was tripled and NO production was multiplied by 1/3. Two simulations were modeled: a) only venular endothelium was considered to be uncoupled, and b) both arteriolar and venular endothelia were considered uncoupled. Resulting concentration profiles are seen in figures 2, 3, and 4 for NO, superoxide, and peroxynitrite, respectively.

Concentrations of NO were drastically affected in both cases. Significant decreases in values occurred at

multiple (or all) of the four endothelial points, which included the left side of arteriole, right side of arteriole, left side of venule, and right side of venule. In the case of only venular uncoupling, values of these four points were decreased by 0, 6.9, 53, and 56%, from left to right. In the case of both venular and arteriolar uncoupling, these changes became 55, 64, 80, and 74%, from left to right.

Superoxide profiles for both cases were very similar to the base case profiles, varying only in height of concentration peaks, which were all located in the endothelial regions. Uncoupling of the venule produced small increases of 0, 1.2, 7.0, and 6.9%, from left to right. In the case of both the arteriole and venule being uncoupled, changes were greater, equaling +10, +12, -60, and -61%, from left to right. Concentration profiles for peroxynitrite follow the same general curve as the base case but again values at the four endothelial points are decreased. For just the uncoupled venule, changes in concentration from the base case equal 0, -6.8, -42, and -46%, from left to right. With uncoupling occurring in both the venule and the arteriole, changes equal -45, -56, -84, and -81%, from left to right.

Discussion of uncoupled eNOS. There was a significant decrease of NO concentration values in the cases of uncoupled NOS. In the case of both arteriolar and venular uncoupling, the concentration profile never exceeded that of the steady-state value reached in the parenchymal tissue. This argues that heightened superoxide levels act to consume the majority of available NO across all regions of the vasculature. Only in the distant tissue was an effect not seen. It is very significant that when only the venular eNOS is uncoupled, a NO decrease of 6.9% was seen in the arteriole endothelium. As literature has shown the ability of venular produced NO to increase arteriole NO concentrations (Guzik et al., 2002; Kavdia, 2006), our model suggests that superoxide produced in the venule can indirectly affect the neighboring arteriole and decrease NO concentrations in the arteriolar endothelium. Thus, venular endothelial dysfunction can impair not just venular dilation but arteriolar dilation as well.

Importance and conclusion. The model has shown that the uncoupling of eNOS can be a significant factor in endothelial dysfunction and reduced NO. One aspect of endothelial dysfunction that was not included in this model was the percentage of eNOS that was uncoupled. BH_4, the cofactor of eNOS, can be oxidized by both superoxide and peroxynitrite (Li and Shah, 2004) and results in uncoupled eNOS. Our model simulation of uncoupled eNOS considered all nitric oxide synthase to be uncoupled but in actual human vasculature, the percentage of eNOS that is uncoupled depends upon the percentage of oxidized BH_4 due to oxidative stress.

Conditions of increased oxidative stress, with little or no effect on NO levels could actually indirectly decrease NO availability in the vasculature by oxidizing BH_4 and uncoupling eNOS, which was seen to decrease NO levels in all regions. This is especially significant to consider since the case of venular uncoupling reduced NO in both the venule and arteriole. Taking into account the oxidation of BH_4, pathological conditions that raise oxidative stress levels in only the venule could indirectly lower NO levels in both the venule and arteriole through uncoupling of venular eNOS. Including oxidized BH_4 percentages in our model could be a significant addition and provide a more complete understanding of these chemical reactions.

In conclusion, numerous studies have experimentally reported changes in interactions of NO, O_2^-, $ONOO^-$, SOD, CO_2, and uncoupled eNOS during different pathophysiological conditions (Bitar et al., 2005; Cannon 1998; Li and Shah, 2004; Mombouli and Vanhoutte, 1999; Taniyama and Griendling, 2003; Wood et al., 2006). Our model has demonstrated these interactions and provided insight into their possible mechanisms. This understanding is significant to future studies of endothelial and vascular dysfunction, and could potentially lead to improved prevention and treatment of many pathological conditions.

LITERATURE CITED

Bitar, M.S., S. Wahid, S. Mustafa, E. Al-Saleh, G.S. Dhaunsi, and F. Al-Mulla. 2005. Nitric oxide dynamics and endothelial dysfunction in type II model of genetic diabetes. Eur J Pharmacol. 511(1): p. 53-64.

Boegehold, M.A. 1996. Shear-dependent release of venular nitric oxide: effect on arteriolar tone in rat striated muscle. Am J Physiol. 271(2 Pt 2): p. H387-95.

Buerk, D.G., K. Lamkin-Kennard, and D. Jaron. 2003. Modeling the influence of superoxide dismutase on superoxide and nitric oxide interactions, including reversible inhibition of oxygen consumption. Free Radic Biol Med. 34(11): p. 1488-503.

Cannon, R.O., 3rd. 1998. Role of nitric oxide in cardiovascular disease: focus on the endothelium. Clin Chem. 44(8 Pt 2): p. 1809-19.

Carlsen, E. and J.H. Comroe, Jr. 1958. The rate of uptake of carbon monoxide and of nitric oxide by normal human erythrocytes and experimentally produced spherocytes. J Gen Physiol. 42(1): p. 83-107.

Cook, S. 2006. Coronary artery disease, nitric oxide and oxidative stress: the "Yin-Yang" effect—a Chinese concept for a worldwide pandemic. Swiss Med Wkly. 136(7-8): p. 103-13.

Ellsworth, M.L., A.S. Popel, and R.N. Pittman. 1988. Assessment and impact of heterogeneities of convective oxygen transport parameters in capillaries of striated muscle: experimental and theoretical. Microvasc Res. 35(3): p. 341-62.

Fridovich, I. 1995. Superoxide radical and superoxide dismutases. Annu Rev Biochem. 64: p. 97-112.

Guzik, T.J., N.E. West, R. Pillai, D.P. Taggart, and K.M. Channon. 2002. Nitric oxide modulates superoxide release and peroxynitrite formation in human blood vessels. Hypertension. 39(6): p. 1088-94.

Haas, T.L. and B.R. Duling. 1997. Morphology favors an endothelial cell pathway for longitudinal conduction within arterioles. Microvasc Res. 53(2): p. 113-20.

Harrison, D.G., J. Widder, I. Grumbach, W. Chen, M. Weber, and C. Searles. 2006. Endothelial mechanotransduction, nitric oxide and vascular inflammation. J Intern Med. 259(4): p. 351-63.

Huie, R.E. and S. Padmaja. 1993. The reaction of no with superoxide. Free Radic Res Commun. 18(4): p. 195-9.

Kavdia, M. 2006. A computational model for free radicals transport in the microcirculation. Antioxid Redox Signal. 8(7-8): p. 1103-11.

Kavdia, M. and A.S. Popel. 2006. Venular endothelium-derived NO can affect paired arteriole: a computational model. Am J Physiol Heart Circ Physiol. 290(2): p. H716-23.

Kavdia, M. and A.S. Popel. 2004. Contribution of nNOS- and eNOS-derived NO to microvascular smooth muscle NO exposure. J Appl Physiol. 97(1): p. 293-301.

Kavdia, M. and A.S. Popel. 2003. Wall shear stress differentially affects NO level in arterioles for volume expanders and Hb-based O2 carriers. Microvasc Res. 66(1): p. 49-58.

Kavdia, M., N.M. Tsoukias, and A.S. Popel. 2002. Model of nitric oxide diffusion in an arteriole: impact of hemoglobin-based blood substitutes. Am J Physiol Heart Circ Physiol. 282(6): p. H2245-53.

Lewis, R.S. and W.M. Deen. 1994. Kinetics of the reaction of nitric oxide with oxygen in aqueous solutions. Chem Res Toxicol. 7(4): p. 568-74.

Li, J.M. and A.M. Shah. 2004. Endothelial cell superoxide generation: regulation and relevance for cardiovascular pathophysiology. Am J Physiol Regul Integr Comp Physiol. 287(5): p. R1014-30.

Malinski, T., Z. Taha, S. Grunfeld, S. Patton, M. Kapturczak, and P. Tomboulian. 1993. Diffusion of nitric oxide in the aorta wall monitored in situ by porphyrinic microsensors. Biochem Biophys Res Commun. 193(3): p. 1076-82.

Mombouli, J.V. and P.M. Vanhoutte. 1999. Endothelial dysfunction: from physiology to therapy. J Mol Cell Cardiol. 31(1): p. 61-74.

Nalwaya, N. and W.M. Deen. 2003. Analysis of cellular exposure to peroxynitrite in suspension cultures. Chem Res Toxicol. 16(7): p. 920-32.

Nellore, K. and N.R. Harris. 2004. Nitric oxide measurements in rat mesentery reveal disrupted venulo-arteriolar communication in diabetes. Microcirculation. 11(5): p. 415-23.

Pfeiffer, S., A.C. Gorren, K. Schmidt, E.R. Werner, B. Hansert, D.S. Bohle, and B. Mayer. 1997. Metabolic fate of peroxynitrite in aqueous solution. Reaction with nitric oxide and pH-dependent decomposition to nitrite and oxygen in a 2:1 stoichiometry. J Biol Chem. 272(6): p. 3465-70.

Popel, A.S. 1989. Theory of oxygen transport to tissue. Crit Rev Biomed Eng. 17(3): p. 257-321.

Radi, R. 1998. Peroxynitrite reactions and diffusion in biology. Chem Res Toxicol. 11(7): p. 720-1.

Rojas, A., H. Figueroa, L. Re, and M.A. Morales. 2006. Oxidative stress at the vascular wall. Mechanistic and pharmacological aspects. Arch Med Res. 37(4): p. 436-48.

Shinozaki, K., A. Kashiwagi, Y. Nishio, T. Okamura, Y. Yoshido, M. Masada, N. Toda, and R. Kikkawa. 1999. Abnormal biopterin metabolism is a major cause of impaired endothelium-dependent relaxation through nitric oxide/O_2^- imbalance in insulin-resistant rat aorta. Diabetes. 48(12): p. 2437-45.

Taniyama, Y. and K.K. Griendling. 2003. Reactive oxygen species in the vasculature: molecular and cellular mechanisms. Hypertension. 42(6): p. 1075-81.

Tsoukias, N.M., M. Kavdia, and A.S. Popel. 2004. A theoretical model of nitric oxide transport in arterioles: frequency- vs. amplitude-dependent control of cGMP formation. Am J Physiol Heart Circ Physiol. 286(3): p. H1043-56.

Vasquez-Vivar, J., B. Kalyanaraman, P. Martasek, N. Hogg, B.S. Masters, H. Karoui, P. Tordo, and K.A. Pritchard Jr. 1998. Superoxide generation by endothelial nitric oxide synthase: the influence of cofactors. Proc Natl Acad Sci U. S. A.. 95(16): p. 9220-5.

Vaughn, M.W., L. Kuo, and J.C. Liao. 1998. Estimation of nitric oxide production and reaction rates in tissue by use of a mathematical model. Am J Physiol. 274(6 Pt 2): p. H2163-76.

Wood, K.C., R.P. Hebbel, D.J. Lefer, and D.N. Granger. 2006. Critical role of endothelial cell-derived nitric oxide synthase in sickle cell disease-induced microvascular dysfunction. Free Radic Biol Med. 40(8): p. 1443-53.

Zacharia, I.G. and W.M. Deen. 2005. Diffusivity and solubility of nitric oxide in water and saline. Ann Biomed Eng. 33(2): p. 214-22.

Table 1: Model Parameters

Parameter	*Value*	*Units*	*Reference*
Systemic Hematocrit	45	%	Text
Capillary Hematocrit	30	%	Text
O_2 concentration	27	μM	Popel, 1989
SOD concentration	1 (0.1)	μM	Buerk et al., 2003
CO_2 concentration	1.14 (0.114)	mM	
Q_{NO}, half of NO release	2.65×10^{-12}	mol/cm^2-s	Vaughn et al., 1998
Q_{sup}, half of O_2^- release	0.2 (2) x Q_{NO}	mol/cm^2-s	Text
D_{NO}	3.3×10^{-5}	cm^2/s	Zacharia and Deen, 2005
D_{sup}	2.8×10^{-5}	cm^2/s	Nalwaya and Deen, 2003
D_{per}	2.6×10^{-5}	cm^2/s	Nalwaya and Deen, 2003
f in tissue	0.640		Text
f in blood	0.817		Text
Uncoupled eNOS NO release	1/3 x Q_{NO}	mol/cm^2-s	Shinozaki et al., 1999
Uncoupled eNOS O_2^- release	3 x Q_{sup}	mol/cm^2-s	Vasquez-Vivar et al., 1998
Geometry:			
Arteriole radius	25	μm	Text
Venule radius	50	μm	Text
Distance between centers	100	μm	Text
Art Cell Free thickness	4.5	μm	Rojas et al., 2006
Ven Cell Free thickness	2.0	μm	
Endothelium thickness	0.5	μm	Wood et al., 2006
Interstitial Space thickness	0.5	μm	Kavdia et al., 2002
Smooth Muscle thickness	6.0	μm	Haas and Duling, 1997
NPT thickness	5.0	μm	Kavdia and Popel, 2006
NO reaction rates:			
NO + O_2 : k_{O2} $-k_{O2}C_{NO}^2C_{O2}$	9.6×10^6	M^{-2}s^{-1}	Lewis and Deen, 1994
NO + O_2^- : k_{perp} $- k_{perp}C_{NO}C_{O2-}$	6.7×10^9	M^{-1}s^{-1}	Huie and Padmaja, 1993
NO + sGC : k_{sm} $- k_{sm}C_{NO}^2$	5×10^4	M^{-1}s^{-1}	Vaughn et al., 1998
NO + RBC	1.4×10^5	M^{-1}s^{-1}	Carlsen and Comroe, 1958
NO + RBC in CR: k_{cr} $- k_{cr}C_{NO}$	1270	s^{-1}	Text
NO in capillaries: k_{cap}	12.4	M^{-1}s^{-1}	Text

$NO + ONOO^- : k_{per}$ $-k_{per}C_{NO}fC_{per}$	9.1×10^4	$M^{-1}s^{-1}$	Pfeiffer et al., 1997
O_2^- reaction rates:			
$O_2^- + SOD: k_{SOD}$ $-k_{SOD}C_{O2}\text{-}C_{SOD}$	1.6×10^9	$M^{-1}s^{-1}$	Fridovich, 1995
$ONOO^-$ reaction rates:			
$ONOO^- + CO_2 : k_{CO2}$ $-k_{CO2}C_{CO2}fC_{per}$	5.6×10^4	$M^{-1}s^{-1}$	Radi, 1998

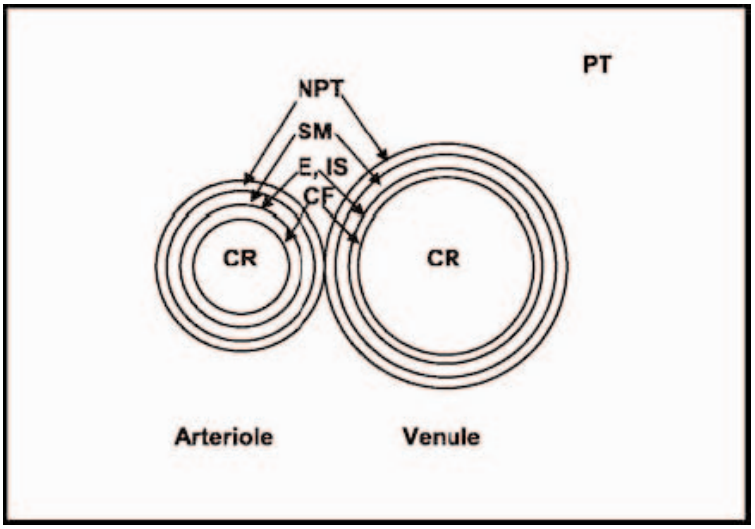

Fig. 1. Model Geometry
The model area includes the arteriole and venule pair, surrounded by parenchymal tissue (PT) containing capillaries. Both the arteriole and venule have a cell-rich (CR) and cell-free (CF) region referring to the presence or absence of red blood cells in the lumen; endothelium (E); interstitial space (IS) between the endothelium and smooth muscle layers; smooth muscle (SM); and a nonperfused parenchymal tissue (NPT), which contains no capillaries. Figure is taken from Kavdia and Popel (2006).

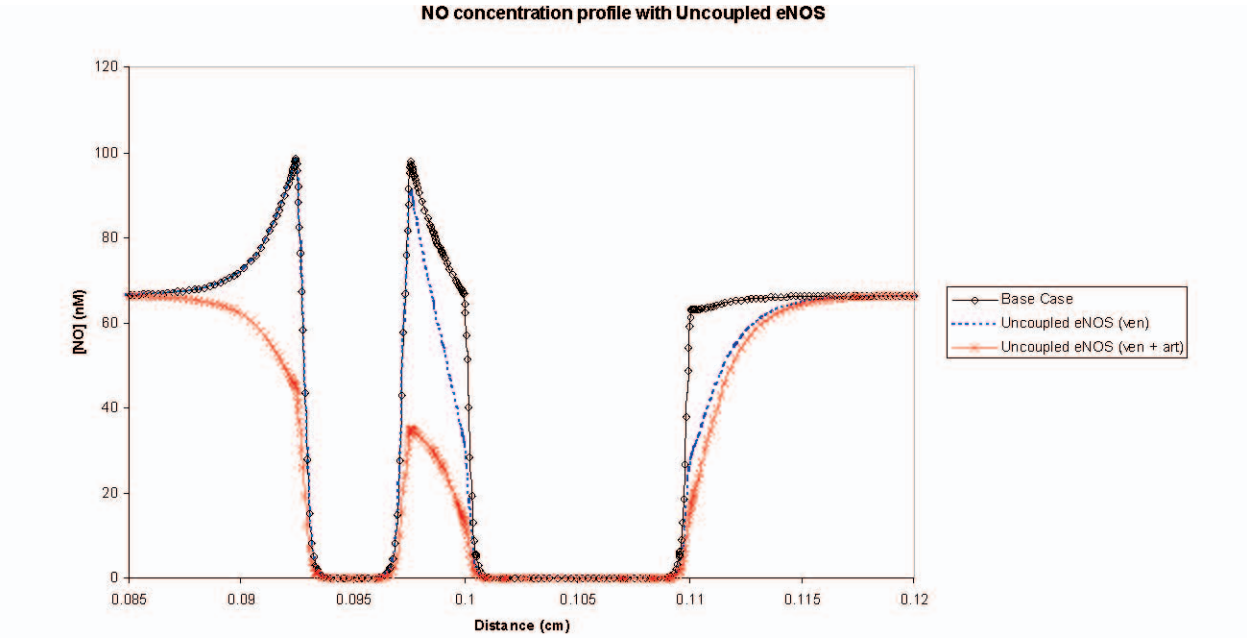

Fig. 2. Effect of uncoupled eNOS on NO profile. To investigate the effect of uncoupled nitric oxide synthase on the species profiles, the parameters for endothelial NO and superoxide production were altered. For the simulation, 1/3 x normal NO release and 3 x normal superoxide release were used in two cases: a) just the venular endothelium, and b) both venular and arteriolar endothelium.

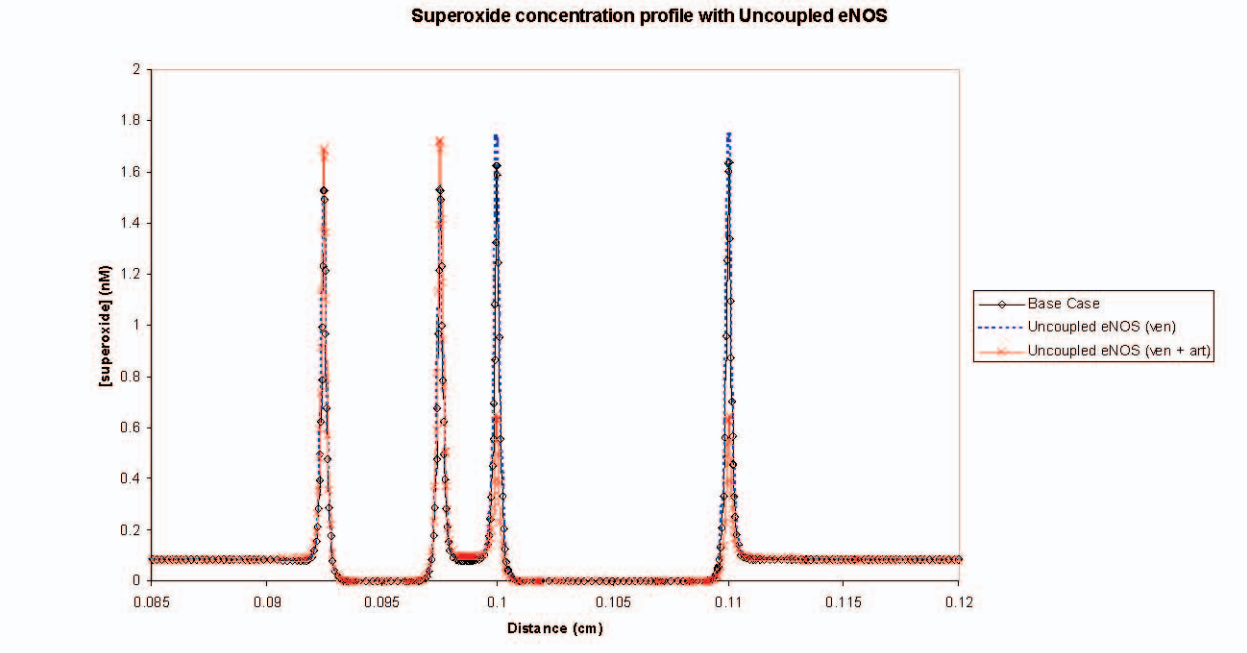

Fig. 3. Effect of uncoupled eNOS on O_2^- profile.

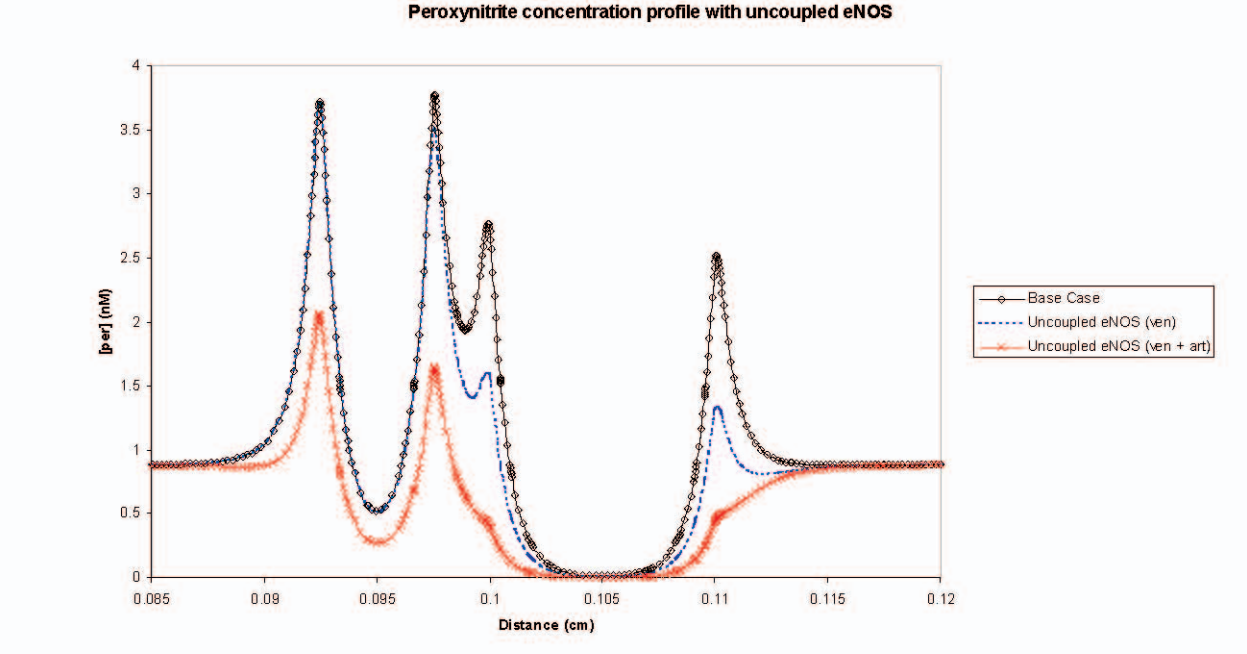

Fig. 4. Effect of uncoupled eNOS on $ONOO^-$ profile.